A Textile Proximity/Pressure Dual-Mode Sensor Based on Magneto-Straining and Piezoresistive Effects

Weiguan Zhang, Qinhua Guo, Yu Duan, Chenyang Xing, and Zhengchun Peng

***Abstract*—The demand for flexible tactile sensors with both contact and contactless sensing capabilities is growing rapidly in the fields of smart robotics and prosthesis. However, it is still a challenge to integrate high performance proximity and pressure sensing functions in one sensor through simple fabrication process. Here, we propose a textile-based dual-mode sensor that can work on both magneto-straining mode (proximity) and piezoresistive mode (pressure). The sensor is simply fabricated by coating two functional materials in a concentric pattern, i.e., a magnetic layer followed by a conductive layer made of 2D MXene composite, on spandex substrate. As the dual-mode sensor approaches to a magnetic object, the attractive magnetic force will stretch the magnetic layer, along with the conductive layer. The strained conductive layer causes an increase of the resistance. Upon contact, the magnetic force reaches its maximum, while the pressure force works against the magnetic force and starts to reduce the strain of the conductive layer, leading to a decrease of the resistance. The turning point of the resistance can be used to identify the contact moment, and as an indicator of the switching of the two working modes of the sensor. Benefitting from the superior conductivity of the MXene material in the conductive layer, high sensitivity for both proximity sensing (13.76 mm^{-1}) and pressure sensing (0.7 kPa^{-1}) was achieved. The proposed dual-mode sensing methodology has great potential in human-machine interaction (HMI) applications.**

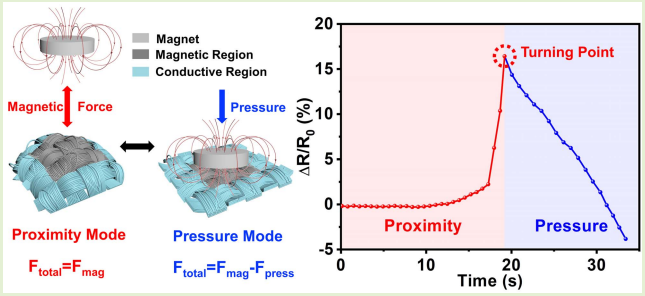

***Index Terms*—Magneto-straining, piezoresistive effect, dual-mode sensor, textile-based sensor, proximity sensing, pressure sensing.**

I. Introduction

ELECTRONIC skin (E-skin) with multifunctional sensing capabilities plays an important role in smooth manipulation and natural human-machine interactions of smart robotics and prosthesis [1], [2]. Till now, lots of flexible tactile sensors including pressure, strain, temperature, humidity, etc. have been proposed based on different sensing mechanisms [3]–[8]. To achieve multimodal tactile perception on e-skin, the most general approach is hybrid integration scheme that assembles multiple sensors on a common flexible substrate individually with a signal recording system [9]–[12]. However, such scheme would significantly decrease the spatial resolution of each sensing function owing to the discrete distribution of sensors on limited space of e-skin. Also, the circuit design for proper signal decoupling and noise isolation becomes more complicated. Thus, incorporating multimode sensing capabilities in one sensor proves to be a promising alternative. Recently, lots of work have been done on developing dual-mode sensors by taking advantage of advanced functional materials or sensing mechanisms to realize distinguishable outputs under different stimuli [13]–[16].

Among all different tactile proception, proximity and pressure are strongly complementary with each other as they are included in the entire process of an object from approaching to contact and press. Seamless monitoring of this pair of parameters is essential for precise control of robotics and prosthesis, especially when they perform certain tasks that

Manuscript received March 26, 2022; accepted April 13, 2022. Date of publication April 18, 2022; date of current version May 31, 2022. This work was supported in part by the Shenzhen Science and Technology Program under Grant JCYJ20190808142609414, Grant JCYJ20200109114237902, Grant KQTD20170810105439418, and Grant JCYJ20200109105212568; in part by the Joint Program of Guangdong Department of Science and Technology and Hong Kong Innovation and Technology Fund under Grant 2021A0505110015; and in part by the National Natural Science Foundation of China under Grant 61904112. The associate editor coordinating the review of this article and approving it for publication was Dr. Cheng-Yao Lo. *(Weiguan Zhang and Qinhua Guo are co-first authors.) (Corresponding author: Zhengchun Peng.)*

Weiguan Zhang is with the College of Mechatronics and Control Engineering, Shenzhen University, Shenzhen 518060, China (e-mail: zhangweiguan@yeah.net).

Qinhua Guo, Yu Duan, Chenyang Xing, and Zhengchun Peng are with the Centre for Stretchable Electronics and Nano-Sensors, College of Physics and Optoelectronic Engineering, Shenzhen University, Shenzhen 518060, China (e-mail: 1900453031@email.szu.edu.cn; duanlinkyu@163.com; xingchenyang319@163.com; zcpeng@szu.edu.cn).

Digital Object Identifier 10.1109/JSEN.2022.3168068

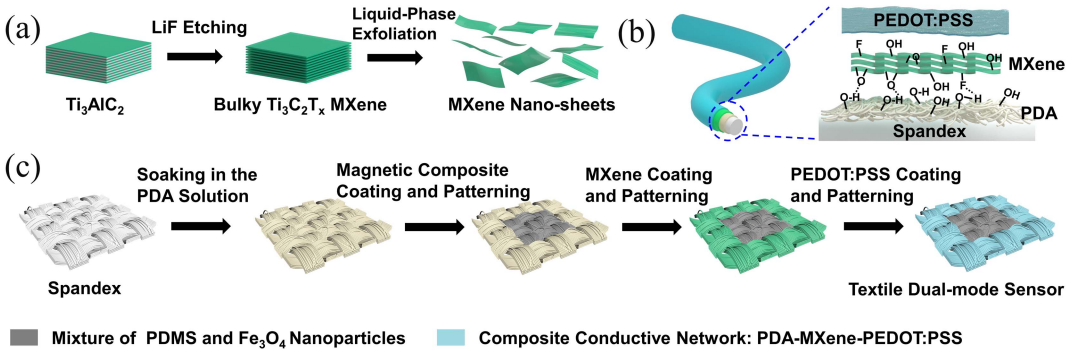

Fig. 1. (a) Preparation of MXene nano-sheets. (b) Schematic drawing of the spandex yarns modified by PDA/MXene/PEDOT: PSS. (c) Fabrication process of the textile proximity/pressure dual-mode sensor.

require collaboration with human. As body parts of human move randomly, proximity information can help robots to avoid unnecessary collision and adjust the path of action timely. Then, the contact force information from pressure sensing mode facilitates the robot to work at adaptive pressures. The demand of human-like operation of robots requires both sensing modes.

Apart from the safe and dexterours control of collaborative robots, proximity/pressure dual-mode sensing technology can also be applied for motion-sensing in virtual and augmented reality scenarios [17], [18]. By wearing our dual-mode sensors on body, a terminal system can capture the motion and gesture state of the player, leading it to precisely implement corresponding actions in virtual or augmented reality. Thus, the dual-mode proximity/pressure sensing is imperative for intelligent human-machine interactions [19]–[21]. Electrostatic coupling effect has been widely used for making proximity/pressure sensors owing to the inherent bidirectional capacitance change caused by the charged object from approaching to pressing, which is appropriate for dual-mode sensing. Zhang *et al.* [22] proposed an orthogonally patterned capacitive sensor array for dual functional sensing. Both proximity, contact, and pressure-loading status can be recognized according to the change of capacitance. However, accuracy for the proximity sensing will be largely affected by other irrelevant charged objects in the sensing region, as well as environmental factors, like humidity and air flow [23]. As an alternative, magnetic-type sensors which have been widely used for navigation and position detection own ultrahigh specificity to magnetic materials and less disturbance factors from environment that benefits to high signal-to-noise ratio. Thus, lots of flexible proximity sensors have been proposed based on the hall effect, magneto-piezoresistive effect, and giant magnetoresistance (GMR) effect [24]– [27], and recently, Ge *et al.* [28] has employed the GMR effect to achieve dual-mode proximity and pressure sensing abilities with superior resolution. However, the significantly raised fabrication complexity and time consumption on making GMR sensors restrict their wide applications. Thus, it is highly demanded to develop flexible proximity/pressure dual-mode sensors with simple fabrication process and high sensitivity.

In this work, we report a novel textile dual-mode sensor based on magneto-straining and piezoresistive effects for continuous proximity and pressure detection. The proposed sensor is simply fabricated by coating magnetic and conductive materials on spandex substrate in a concentric square pattern. The working mechanism for dual-mode sensing relies on the change of the total force exerted on the sensor from approaching to pressing of a magnetic object causing a bidirectional resistance change, and the turning point on the resistance change can be used to distinguish the switching of the two modes. Effect of MXene sheets embedded in the composite conductive material was first studied. Then, concentration of Fe_3O_4 nanoparticles in making the magnetic composite was modified and tunable sensitivity of the dual-mode sensor for both proximity (1.53-13.76 mm^{-1}) and pressure (0.11-0.7 kPa^{-1}) were achieved. The fabricated textile-based dual-mode sensor has been successfully applied for real-time recording of handshake between human and robot as well as gait monitoring for smart prosthesis, proving its great potential for intelligent human-machine interactions.

II. Experimental Details

A. Materials Preparation

Commercial spandex with excellent elasticity is selected as the flexible substrate without any chemical treatment. The magnetic composite was prepared by adding Fe_3O_4 nanoparticles (200 nm diameter, Macklin Biochemical Co., Ltd.) into polydimethylsiloxane (PDMS) (Sylgard 184, Dow Corning) which was made by using 10:1 weight mixing ratio of elastomer and curing agent. After fully stirring at room temperature for 10 min and degassing in vacuum chamber for 15 min, the Fe_3O_4 nanoparticles were distributed uniformly in the PDMS, and the magnetic composite was ready prepared.

Then, the $Ti_3C_2T_x$ MXene nano-sheets were fabricated by chemical etching method [29]. The process is drawn in Fig. 1(a). 2 g LiF powder was added in 40 mL hydrochloric acid solution (9M) and stirred for 30 min at room temperature to obtain the etching solution. Then, 2 g Ti_3AlC_2 powder (200 mesh, 11 Technology Co., Ltd.) was added into the etching solution slowly and the mixture was continuously stirred for 24 h at the speed of 600 rpm under 35 °C. Aluminum layers were all etched, and stacked bulky $Ti_3C_2T_x$ was obtained after several cycles of deacidification using deionized water. By dispersing the bulky MXene in ethyl alcohol for 1 h ultrasonic, the required MXene solution with nano-sheets was obtained

by replacing deionized water as the solvent. Dopamine solution was made by putting 0.4 g dopamine powder and 0.24 g Tris-HCl powder in 200 ml deionized water. Poly (3,4-ethylenedioxythiophene) polystyrene sulfonate (PEDOT: PSS) ink was a product from Orgacon (EL-P3165).

B. Sensor Fabrication and Characterization

The spandex was first cleaned by ethanol and deionized water, and then, cut into pieces with 3 × 3 cm^2 dimension. Immerged in dopamine solution for 6 hours at 25 °C, the yarns of spandex pieces were deposited with polydopamine (PDA). Then, the modified spandex pieces were washed with deionized water 3 times. After drying, the as-prepared magnetic composite was brushed on the center of the spandex substrate through a patterned polyethylene terephthalate (PET) mask with an opening square of 1 × 1 cm^2 and thickness of 0.5 mm. Heated on a hotplate at 80 °C for 4 h, the magnetic composite was fully cured. Then, MXene solution was dip-coated on the rest area of the substrate around the magnetic region and dried at 80 °C in nitrogen. The MXene-PDA-spandex area was then coated with PEDOT: PSS ink defined by another PET mask. Schematic drawing of the modified conductive yarns is shown in Fig. 1(b). PDA can firmly adhere to the surface of yarns and bond with MXene through hydrogen bonds [30], then, owing to the excellent formability and conductivity, PEDOT: PSS ink is employed as the encapsulation layer that clamps the MXene sheets stably on the yarns and maintains the electrical conduction under stretching or bending of the sensor. After drying the PEDOT: PSS ink in nitrogen at 100 °C for 3 h, the textile-based dual-mode sensor was obtained and the fabrication process is depicted in Fig. 1(c).

Scanning electron microscope (SEM) (Hitachi SU8010) was used for morphology characterization, Energy-dispersive X-ray spectroscopy (EDS) element analysis and mapping of the sensor. The magnetic characteristics of the magnetic composite were measured using SQUID-VSM (MPMS-3, Quantum Design). The dual-mode responses of the sensor were measured by a dynamic fatigue testing system (ElectroPuls 1000, Instron). A magnet with a diameter of 15 mm and field of 220 mT was mounted on the upper gripper of the instrument and its motion was precisely controlled by the system. The real-time resistance of the sensor was recorded by a digital multimeter (Keithley 6500).

III. Results and Discussion

The fabricated textile dual-mode sensor is shown in Fig. 2 (a). The fabrication method adopted in this work enables rapid and batch manufacturing of the sensor with scalable dimensions for different applications. For instance, stencil with higher resolution can be used to fabricate reduced size of the sensors size. Cross-sectional SEM image as well as EDS element mapping of the magnetic region are shown in Fig. 2 (b). The magnetic composite had infiltrated throughout the yarns of the textile and cladded them together firmly, and the total thickness of the sensor is 0.5 mm. This ensures the region behaves as a uniform integrity under the magnetic field. Magnetic hysteresis loop of the magnetic composite (20% w/w

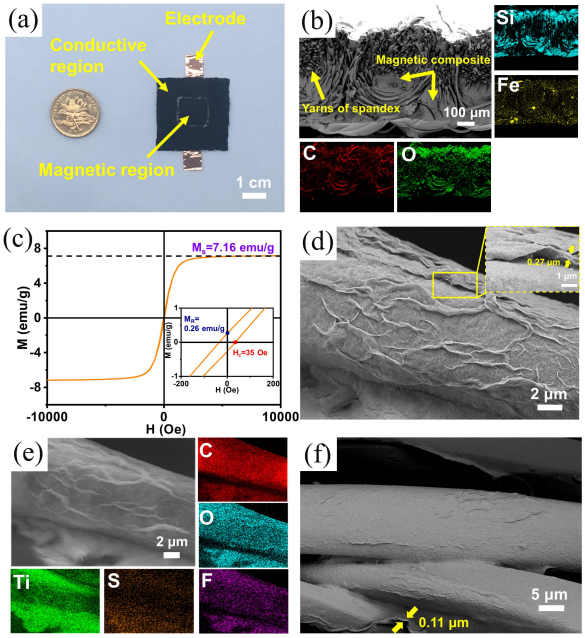

Fig. 2. Characterization of the fabricated textile dual-mode sensor. (a) Photograph of the as-fabricated sensor. (b) Cross-sectional SEM image and EDS element mapping of the magnetic region. (c) Magnetic hysteresis loop of the magnetic composite. (d)-(e) SEM image and EDS element mapping of the conductive yarn. (f) SEM image of the pure MXene layer on the yarn.

Fe_3O_4 nanoparticles) is plotted in Fig. 2(c). The saturation magnetization, remanent magnetization, and coercive field of the magnetic composite are 7.16 emu/g, 0.26 emu/g, and 35 Oe respectively. Also, the magnetic composite demonstrates a ferrimagnetic behavior as shown in the figure. Higher fraction of Fe_3O_4 nanoparticle will result larger magnetic susceptibility which benefits to the proximity sensing, however, also increase the stiffness of the magnetic composite that make it harder to be bent and compressed. In this work, the maximum filling fraction of Fe_3O_4 nanoparticle is set at 20%. SEM image in Fig. 2 (d) shows the conductive region of the sensor modified by PDA/MXene/PEDOT: PSS. It is noted that wrinkles of the composite material on the surface of yarns were formed, which is mainly attributed to the repeated heating and cooling in sensor fabrication. Besides, inset in Fig. 2(d) illustrates the overlapping of the wrinkled materials caused by the thermal stress. The stacked wrinkling layers can benefit to the sensitivity of pressure mode. Also, thickness of the conductive composite layer is 0.27 μm. EDS element mapping of the conductive yarn in Fig. 2(e) demonstrates its entire surface with wrinkling layers contains MXene and PEDOT: PSS, proving the successful compositing of the conductive material. Thickness of the MXene layer is 0.11 μm, as individually prepared and measured in Fig. 2(f).

In this work, embedded MXene sheets can reduce the resistance of the sensor, and Fig. 3 (a) compares the I-V curve of pure PEDOT: PSS and the composite material that a 500% drop on resistance was achieved. Also, PDA and PEDOT: PSS can sandwich the MXene sheets in the center stably, and the composite conductive material bonds firmly on the yarns of spandex substrate. After 1000 cycles of bending-recovering

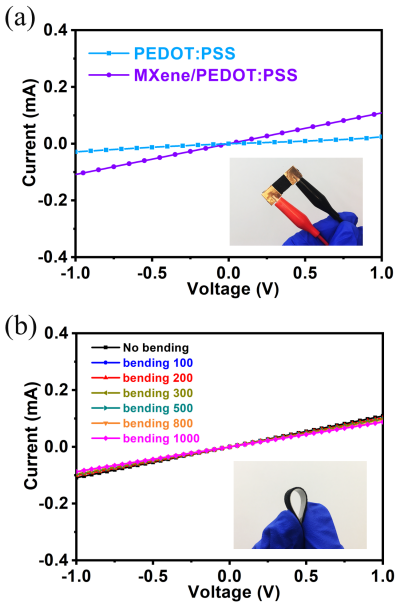

Fig. 3. (a) I-V curves of the conductive spandex with and without MXene. (b) I-V curves of the conductive spandex with different cycles of bending-recovering test.

test, resistance of the composite material shows no significant change in Fig. 3(b). As such, the fabrication methodology we proposed in this work ensures reliable performance of the sensor.

Working principle of the textile dual-mode sensor is schematically drawn in Fig. 4 (a). With the approaching of a magnet, Fe_3O_4 nanoparticles in the magnetic region will be magnetized, and then, the induced magnetic force will stretch the conductive region around. The magnetic force increases with the decrease of approaching distance, and upon contact, the magnetic force reaches its maximum, whereas the reversal pressure force starts to increase, thus, the stretched conductive region will be gradually released, and then, compressed by the magnet. During the process from approach to contact and press, the total force on the sensor increases first, and then decreases.

Finite element simulation was performed to investigate the stress distribution and change on the sensor. Owing to the time and computational cost on the modeling of crossed morphology of textile as well as the conductive composites on the yarns, a simplified model was built to qualitatively analyze the dual-mode sensing principle. From Fig. 4 (b), when the magnet approaches to the sensor, magnetic region in the center induces the stress and behaves as a hinge to transmit the stress to adjoining conductive region. The total force change on the sensor from approaching to press was obtained through surface integration of the stress as plotted in Fig. 4 (c). It is as predicted above that the equivalent force on the dual-mode sensor increases first, and decreases after contact with the magnet. A distinct turning point in the figure indicates the transition of the two sensing modes. Owing to the strain and piezoresistive effect of the conductive yarns, resistance of the sensor changes simultaneously with the force. The embedded MXene sheets on the yarns dominate the resistance change as schematically drawn in Fig. 4 (d). Stretching of the yarns leads to separation of the stacked MXene sheets and increase of the resistance. After contact, reversal compressive pressure releases the stretched yarns gradually and the separated MXene sheets recover to dense connection, so the resistance starts to decrease. Keep pressing the sensor will tighten the connection of MXene sheets and result in further decrease of resistance. Thus, from approaching to contact and press, resistance of the sensor will also increase first, and then decrease, which is consistent with the change of total force on the sensor.

Effect of MXene sheets on sensitivity enhancement was investigated. Compared to the sensor made by pure PEDOT: PSS ink for the conductive region, the proposed dual-mode sensor in this work embedded MXene sheets in the composite conductive material, and the stacked sheets will be pulled away or pushed together when the yarns are stretched or compressed. It will result in much larger resistance change of the sensor which means higher sensitivity for both modes. Fig. 5 (a) compares the relative resistance change of the sensor as a function of approaching distance of the magnetic object. The reference R_0 is the resistance measured at zero magnetic field. Embedded with MXene sheets, sensing distance increased from 1.8 to 3.5 mm, and sensitivity improved about 4 times from 0.32 to 1.53 mm^{-1} when the magnet approaches to the surface of the sensor. Pressure response are also compared in Fig. 5 (b). With external pressure increased from 0 to 100 kPa, sensitivity of the sensor with pure PEDOT: PSS is 0.77 (0−3 kPa) and 0.03 kPa^{-1} (3−100 kPa), while by having MXene, the sensitivity at 5−100 kPa range increased to 0.15 kPa^{-1} which is 5 times larger than the sensor made by pure PEDOT: PSS. Thus, MXene sheets benefit to the performance of the dual-mode sensor.

Concentration of Fe_3O_4 nanoparticles in preparing the magnetic composite was systemically studied by setting it from 10 % to 20 % in step of 5 %. Fig. 6 (a) shows the relative resistance change of the sensors with different Fe_3O_4 nanoparticle concentrations when the approaching distance of the magnet changed from 10 to 0 mm. It is noted that the proximity-mode sensitivity of the sensor increases with the increase of Fe_3O_4 nanoparticle concentration. It can be explained by the increase of induced magnetic force at certain approaching distance that causes larger resistance change of the conductive yarns. By having 20 % Fe_3O_4 nanoparticles, the sensitivity gradually increased from 0.05 (10−3.4 mm) to 0.85 mm^{-1} (3.4−1 mm), and reached to 13.76 mm^{-1} (1−0 mm). The maximum sensitivity appears at the distance range when the magnet approaches to the surface of sensor, and it is ∼224 % and 900% higher than the sensor made by 15% and 10% Fe_3O_4 nanoparticles respectively. On the contrary, the pressure-mode sensitivity decreases with the increase of Fe_3O_4 nanoparticle concentration as shown in Fig. 6 (b). It is mainly attributed to the stiffness increase of the magnetic region by having more Fe_3O_4 nanoparticles that causes less deformation of both magnetic and conductive regions under certain pressure level. Thus, the resistance change of the sensor will decrease. From 0−200 kPa pressure range, the sensor made by 10% Fe_3O_4 nanoparticle concentration shows the highest sensitivity, and the sensitivity decreased

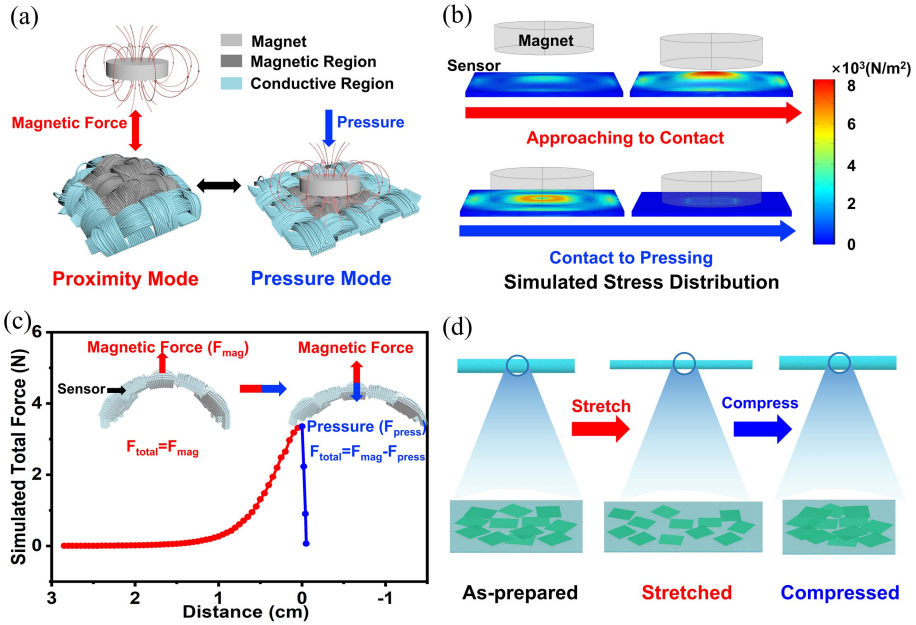

Fig. 4. (a) Schematic drawing of the working principle of the dual-mode sensor. (b) Simulated stress distribution and (c) total force of the sensor from proximity mode to pressure mode. (d) Change of MXene sheets under the two working modes.

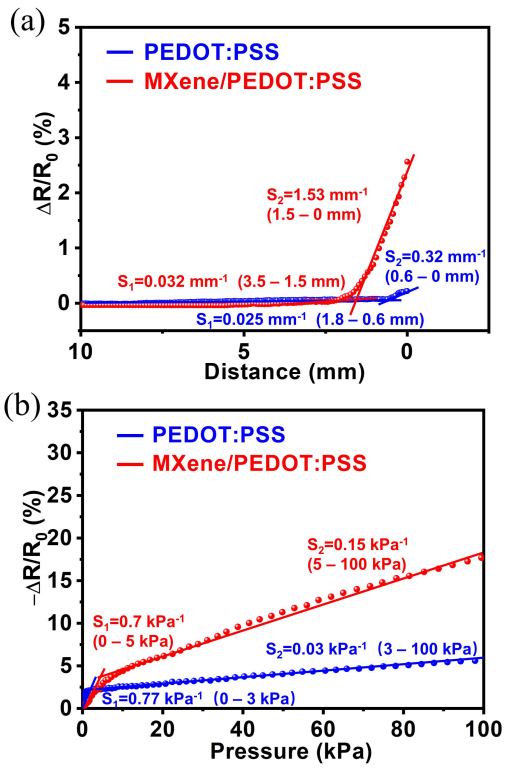

Fig. 5. Measured relative resistance change of the dual-mode sensor made with/without MXene as a function of (a) approaching distance and (b) pressure.

from 0.7 (0−5 kPa) to 0.15 (5−100 kPa), and 0.076 kPa^{-1} (100−200 kPa). The maximum sensitivity of the sensor which is obtained at low-pressure range made by 10 % Fe_3O_4 nanoparticles is ∼184% larger than it with 15 %, and ∼636 % larger than it with 20 %. Tunable sensitivities for both proximity and pressure mode are realized by modifying the Fe_3O_4 nanoparticle concentrations in making the magnetic composite (Fig. 6 (a) and (b)). To realize the dual-mode sensing, the central region of the sensor is designed as non-conductive magnetic composite, thus, the pressure sensitivity of our sensor is lower than MXene/textile sensors designed with full region for single mode pressure sensing [29], [31]. We compared the sensitivity of our sensor with previously reported dual-mode proximity/pressure sensors using different sensing mechanisms in Table I [22], [32]–[34]. The results reveal that the performance of our sensor stands out among these comparable works.

TABLE I
COMPARISON OF REPORTED DUAL-MODE PROXIMITY/PRESSURE SENSORS

No.	Working principle	Sensitivity		Ref.
		Proximity	Pressure	
1	Capacitive/triboelectric	0.04 cm^{-1}	1.04 V/kPa	[32]
2	Inductive/Capacitive	3.7 cm^{-1}	5.57×10^{-4} kPa^{-1}	[33]
3	Capacitive/Capacitive	6.25 cm^{-1}	4 ×10^{-4} kPa^{-1}	[22]
4	Capacitive/Capacitive	11 cm^{-1}	0.198 kPa^{-1}	[34]
5	Magneto-straining and piezoresistive	15.3-137.6 cm^{-1}	0.11-0.7 kPa^{-1}	This work

We also studied the performance of the sensor under bending conditions. Results in Fig. 7 (a) and (b) compare the proximity and pressure sensitivity of the sensor by bending from 0°, to 5°, and 10°. Noted from the figures that the sensor still demonstrates good sensing performance after bent to certain angles, and the reasons for the gradual decrease on sensitivity are mainly attributed to the pre-stretched yarns and reduced compressible area of the sensor on curved surface.

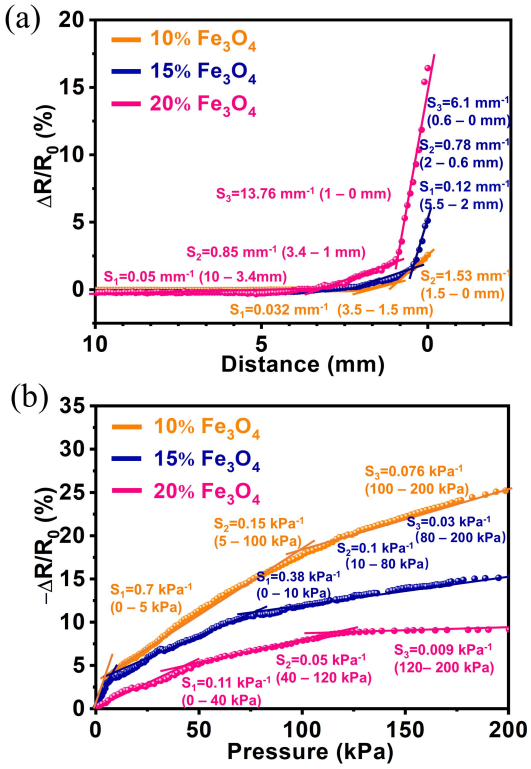

Fig. 6. (a) Proximity and (b) pressure response of the dual-mode sensor using different Fe_3O_4 nanoparticle concentrations.

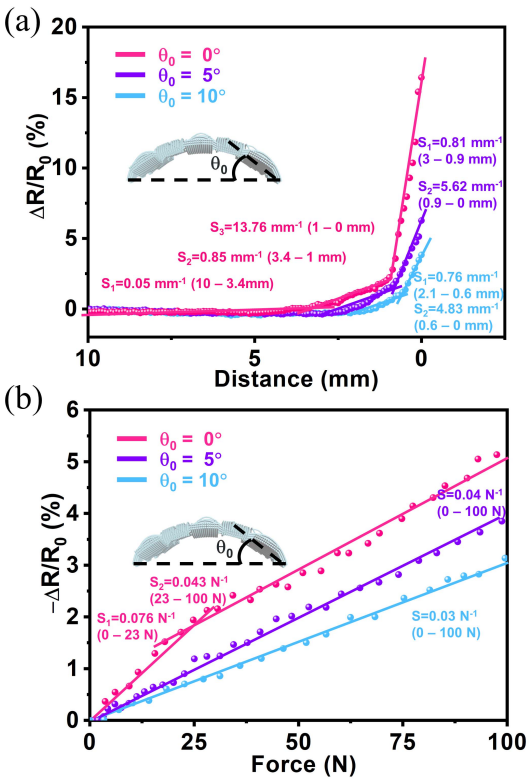

Fig. 7. (a) Proximity and (b) pressure response of the dual-mode sensor under different bending angles.

Thus, both the magnetic force and pressure cause smaller resistance change. With proper selection of Fe_3O_4 nanoparticle concentration and calibration factor for bending angle, our textile dual-mode sensor can be used for different application scenarios according to specific requirements.

Continuous response of the dual-mode sensor to the magnet from approaching to contact and pressing was measured by using the one made by 20% Fe_3O_4 nanoparticles. Relative resistance change of the sensor is shown in Fig. 8 (a), and it increased gradually as the magnet approached from 10 mm away. After contact, the magnet started to press the sensor, and the resistance turned to decrease. The measured response curve in Fig. 8 (a) exhibits the same trend as simulation result in Fig. 4 (c), which verifies our hypothesis on the working mechanism of the textile dual-mode sensor. In addition, a distinct turning point on resistance change can be used to distinguish the proximity mode and pressure mode of the dual-mode sensor under dynamic working condition. Response time of the sensor was characterized by using a custom-made ejection system that allows the instant presenting of a magnet to be driven to approach to and separate from the sensor. Benefitting from the excellent elasticity of spandex and stacked MXene sheets, fast response time of 60 ms was achieved as shown in Fig. 8 (b). Then, the repeatability of the sensor was examined under approaching-separation test at 1 Hz frequency with a magnet at 10 mm above the sensor. Repeated stretching of the textile releases the thermal stress on the yarn and the encapsulation layer, leading to more MXene nanosheets in contact with each other. Hence, the reference resistance of the sensor becomes smaller with increasing cycles of measurement

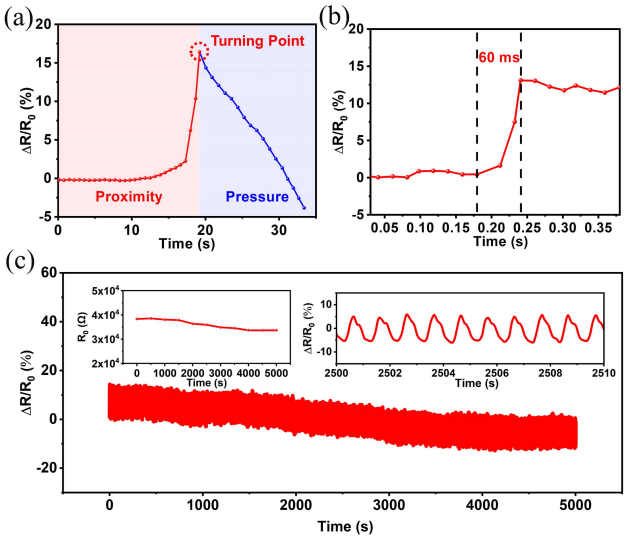

Fig. 8. (a) Real-time response of the dual-mode sensor for continuous proximity and pressure sensing (turning point indicates the transition of the two modes). (b) Response time of the dual-mode sensor. (c) Repeated measurement of approaching-separation test 10 mm above the dual-mode sensor for over 5000 cycles.

(inset of Fig. 8(c)), which results in the drift of the response curve. We note that after ~3000 cycles, the response became pretty stable. Thus, we believe with pre-stretching cycles and proper calibration, our dual-mode sensor can be used in practical applications.

Incorporated with the proximity and pressure sensing functions, the proposed textile dual-mode sensor can be applied for human-machine interactions. Such as service robotics may

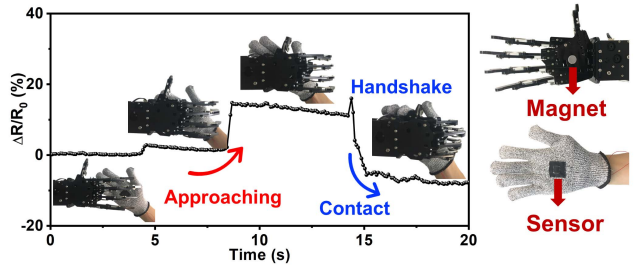

Fig. 9. Continuous monitoring of handshake between the human and robot by the textile dual-mode sensor.

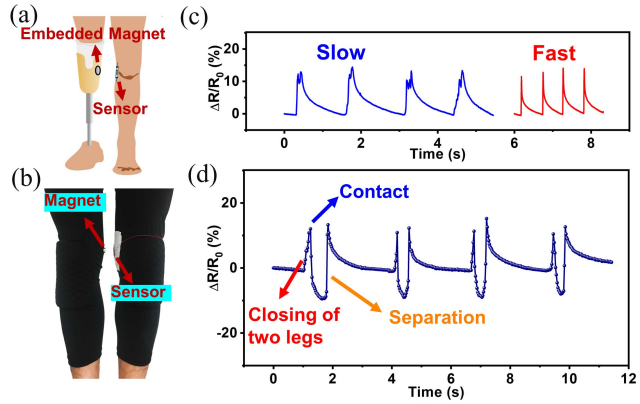

Fig. 10. Demonstration of the textile dual-mode sensor for gait monitoring of prosthetic patient. (a) schematic drawing of the patient wearing the sensor. (b) volunteer mimicking the situation. (c) stride frequency of the "patient". (d) improper gaits of the "patient".

perform certain tasks together with human. Thus, real-time monitoring of their approaching distance and contact pressure during cooperating or touching with human is of high importance for robots to adjust their behavior in advanced and avoid unwanted damage. Fig. 9 demonstrates an action of handshake between human and robot. The process from getting close to contact, and then, shaking hands were all recorded by the dual-mode sensor. With this, the sensor shows great potential to be used in safe and intelligent human-machine interactions. Also, the dual-mode sensor can be used for gait monitoring of prosthetic patients as schematically drawn in Fig. 10 (a). To mimic such scenario, as shown in Fig. 10 (b), a volunteer wore the dual-mode sensor on one leg, and the magnet on the other leg, then performed a series of walking postures. First, different stride frequencies of the "patient" can be detected by the proximity sensing mode as shown in Fig. 10 (c). Also, improper gaits of the "patient" after wearing the prosthesis may lead to extreme small gap distance or even hitting of the two legs, and cause further injury to the patient for long-term usage. Such harmful postures can be monitored by the sensor in real time as illustrated in Fig. 10 (d). In addition, the recorded data can be used to warn the patients timely of the improper gaits. With the successful demonstration of the sensor in the above representative applications, we show that our dual-mode proximity/pressure sensing can facilitate safe and natural collaboration between robots with human. Also, by incorperating two sensing functions on one device, we can achieve high spatial resolution of electronic skin. Thus, the textile dual-mode sensor proposed in this work provides a new prospection for future human-machine interactions.

IV. Conclusion

In this paper, a textile-based proximity/pressure dual-mode sensor was realized by utilizing the magneto-straining and piezoresistive effects. This sensing mechanism allows for high specificity of the sensor that only responds to the target magnetic objects and avoids disturbance from irrelevant factors. Besides, the proximity and pressure working modes can be clearly distinguished by a distinct turning point on the relative resistance change of the sensor. Embedded MXene nanosheets in the composite conductive material enable ultrahigh sensitivity of the dual-mode sensor, and the sensitivity for both proximity and pressure sensing mode can be tuned from 1.53 to 13.76 mm^{-1} and 0.11 to 0.7 kPa^{-1} respectively by changing Fe_3O_4 nanoparticle concentrations in the magnetic composite. Also, a fast response time of 60 ms and repeatable performance with over 5000 cycles of approaching-separation test were demonstrated. We successfully applied the dual-mode sensor as a wearable e-skin for human-machine interactions. More importantly, the design strategy and fabrication process developed in this work are suitable for batch fabrication of the dual-mode sensor.

References

[1] K. Xu, Y. Lu, and K. Takei, "Multifunctional skin-inspired flexible sensor systems for wearable electronics," *Adv. Mater. Technol.*, vol. 4, no. 3, Mar. 2019, Art. no. 1800628, doi: 10.1002/admt.201800628.

[2] S. Yao *et al.*, "Nanomaterial-enabled flexible and stretchable sensing systems: Processing, integration, and applications," *Adv. Mater.*, vol. 32, no. 15, Apr. 2020, Art. no. 1902343, doi: 10.1002/adma.201902343.

[3] L. Huang, H. Wang, D. Zhan, and F. Fang, "Flexible capacitive pressure sensor based on laser–induced graphene and polydimethylsiloxane foam," *IEEE Sensors J.*, vol. 21, no. 10, pp. 12048–12056, May 2021, doi: 10.1109/JSEN.2021.3054985.

[4] W. Zhang *et al.*, "A high-performance flexible pressure sensor realized by overhanging cobweb-like structure on a micropost array," *ACS Appl. Mater. Interfaces*, vol. 12, no. 43, pp. 48938–48947, Oct. 2020, doi: 10.1021/acsami.0c12369.

[5] H. Hwang, Y. Kim, J. Park, and U. Jeong, "2D percolation design with conductive microparticles for low-strain detection in a stretchable sensor," *Adv. Funct. Mater.*, vol. 30, no. 13, Mar. 2020, Art. no. 1908514, doi: 10.1002/adfm.201908514.

[6] L. Xu *et al.*, "A transparent, highly stretchable, solvent-resistant, recyclable multifunctional ionogel with underwater self-healing and adhesion for reliable strain sensors," *Adv. Mater.*, vol. 33, no. 51, Dec. 2021, Art. no. 2105306, doi: 10.1002/adma.202105306.

[7] Y. Zhang and Y. Cui, "Development of flexible and wearable temperature sensors based on PEDOT:PSS," *IEEE Trans. Electron Devices*, vol. 66, no. 7, pp. 3129–3133, Jul. 2019, doi: 10.1109/TED.2019.2914301.

[8] X. Li *et al.*, "Self-powered humidity sensor based on polypyrrole/melamine aerogel for real-time humidity monitoring," *IEEE Sensors J.*, vol. 21, no. 3, pp. 2604–2609, Feb. 2021, doi: 10.1109/JSEN.2020.3027743.

[9] S. Zhao and R. Zhu, "Electronic skin with multifunction sensors based on thermosensation," *Adv. Mater.*, vol. 29, no. 15, Apr. 2017, Art. no. 1606151, doi: 10.1002/adma.201606151.

[10] K. Xu, Y. Lu, and K. Takei, "Flexible hybrid sensor systems with feedback functions," *Adv. Funct. Mater.*, vol. 31, no. 39, Sep. 2021, Art. no. 2007436, doi: 10.1002/adfm.202007436.

[11] Y. Lu *et al.*, "Multimodal plant healthcare flexible sensor system," *ACS Nano*, vol. 14, no. 9, pp. 10966–10975, Sep. 2020, doi: 10.1021/acsnano.0c03757.

[12] Y. Yamamoto *et al.*, "Printed multifunctional flexible device with an integrated motion sensor for health care monitoring," *Sci. Adv.*, vol. 2, no. 11, Nov. 2016, Art. no. e1601473, doi: 10.1126/sciadv.1601473.

[13] Z. Ma, J. Zhang, J. Li, Y. Shi, and L. Pan, "Frequency-enabled decouplable dual-modal flexible pressure and temperature sensor," *IEEE Electron Device Lett.*, vol. 41, no. 10, pp. 1568–1571, Oct. 2020, doi: 10.1109/LED.2020.3020937.
[14] I. You *et al.*, "Artificial multimodal receptors based on ion relaxation dynamics," *Science*, vol. 370, no. 6519, pp. 961–965, Nov. 2020, doi: 10.1126/science.aba5132.
[15] H. Park *et al.*, "Microporous polypyrrole-coated graphene foam for high-performance multifunctional sensors and flexible supercapacitors," *Adv. Funct. Mater.*, vol. 28, no. 33, Aug. 2018, Art. no. 1707013, doi: 10.1002/adfm.201707013.
[16] F. Guan *et al.*, "Silver nanowire–bacterial cellulose composite fiber-based sensor for highly sensitive detection of pressure and proximity," *ACS Nano*, vol. 14, no. 11, pp. 15428–15439, Nov. 2020, doi: 10.1021/acsnano.0c06063.
[17] G. S. C. Bermúdez, H. Fuchs, L. Bischoff, J. Fassbender, and D. Makarov, "Electronic-skin compasses for geomagnetic field-driven artificial magnetoreception and interactive electronics," *Nature Electron.*, vol. 1, no. 11, pp. 589–595, Nov. 2018, doi: 10.1038/s41928-018-0161-6.
[18] M. Ha *et al.*, "Printable and stretchable giant magnetoresistive sensors for highly compliant and skin-conformal electronics," *Adv. Mater.*, vol. 33, no. 12, Mar. 2021, Art. no. 2005521, doi: 10.1002/adma.202005521.
[19] P. F. Zhao *et al.*, "Strain-discriminable pressure/proximity sensing of transparent stretchable electronic skin based on PEDOT:PSS/SWCNT electrodes," *ACS Appl. Mater. Interfaces*, vol. 12, no. 49, pp. 55083–55093, Dec. 2020, doi: 10.1021/acsami.0c16546.
[20] Q. Wang *et al.*, "A dual-trigger-mode ionic hydrogel sensor for contact or contactless motion recognition," *Mater. Horizons*, vol. 7, no. 10, pp. 2673–2682, Oct. 2020, doi: 10.1039/d0mh00862a.
[21] J. Liang, J. Wu, H. Huang, W. Xu, B. Li, and F. Xi, "Soft sensitive skin for safety control of a nursing robot using proximity and tactile sensors," *IEEE Sensors J.*, vol. 20, no. 7, pp. 3822–3830, Apr. 2020, doi: 10.1109/JSEN.2019.2959311.
[22] B. Zhang *et al.*, "Dual functional transparent film for proximity and pressure sensing," *Nano Res.*, vol. 7, no. 10, pp. 1488–1496, Oct. 2014, doi: 10.1007/s12274-014-0510-3.
[23] Y. Ye, C. Zhang, C. He, X. Wang, J. Huang, and J. Deng, "A review on applications of capacitive displacement sensing for capacitive proximity sensor," *IEEE Access*, vol. 8, pp. 45325–45342, 2020, doi: 10.1109/ACCESS.2020.2977716.
[24] B. Ozer, H. Piskin, and N. Akdogan, "Shapeable planar Hall sensor with a stable sensitivity under concave and convex bending," *IEEE Sensors J.*, vol. 19, no. 14, pp. 5493–5498, Jul. 2019, doi: 10.1109/JSEN.2019.2907616.
[25] W. Zhang *et al.*, "Touchless sensing interface based on the magneto-piezoresistive effect of magnetic microstructures with stacked conductive coating," *ACS Appl. Mater. Interfaces*, vol. 13, no. 51, pp. 61422–61433, Dec. 2021, doi: 10.1021/acsami.1c19137.
[26] M. Kondo *et al.*, "Imperceptible magnetic sensor matrix system integrated with organic driver and amplifier circuits," *Sci. Adv.*, vol. 6, no. 4, Jan. 2020, Art. no. eaay6094, doi: 10.1126/sciadv.aay6094.
[27] G. S. C. Bermúdez *et al.*, "Magnetosensitive e-skins with directional perception for augmented reality," *Sci. Adv.*, vol. 4, no. 1, Jan. 2018, Art. no. eaao2623, doi: 10.1126/sciadv.aao2623.
[28] J. Ge *et al.*, "A bimodal soft electronic skin for tactile and touchless interaction in real time," *Nature Commun.*, vol. 10, no. 1, p. 4405, Sep. 2019, doi: 10.1038/s41467-019-12303-5.
[29] Y. Guo, M. Zhong, Z. Fang, P. Wan, and G. Yu, "A wearable transient pressure sensor made with MXene nanosheets for sensitive broad-range human–machine interfacing," *Nano Lett.*, vol. 19, no. 2, pp. 1143–1150, Feb. 2019, doi: 10.1021/acs.nanolett.8b04514.
[30] M. Gong *et al.*, "Knittable and sewable spandex yarn with nacre-mimetic composite coating for wearable health monitoring and thermo- and antibacterial therapies," *ACS Appl. Mater. Interfaces*, vol. 13, no. 7, pp. 9053–9063, Feb. 2021, doi: 10.1021/acsami.1c00864.
[31] L. Yang *et al.*, "Wearable pressure sensors based on MXene/tissue papers for wireless human health monitoring," *ACS Appl. Mater. Interfaces*, vol. 13, no. 50, pp. 60531–60543, Dec. 2021, doi: 10.1021/acsami.1c22001.
[32] C. Zhang, S. Liu, X. Huang, W. Guo, Y. Li, and H. Wu, "A stretchable dual-mode sensor array for multifunctional robotic electronic skin," *Nano Energy*, vol. 62, pp. 164–170, Aug. 2019, doi: 10.1016/j.nanoen.2019.05.046.
[33] H. Seung Han *et al.*, "A highly sensitive dual mode tactile and proximity sensor using carbon microcoils for robotic applications," in *Proc. IEEE Int. Conf. Robot. Autom. (ICRA)*, Stockholm, Sweden, May 2016, pp. 97–102.
[34] M. R. Kulkarni *et al.*, "Transparent flexible multifunctional nanostructured architectures for non-optical readout, proximity, and pressure sensing," *ACS Appl. Mater. Interfaces*, vol. 9, no. 17, pp. 15015–15021, May 2017, doi: 10.1021/acsami.6b16840.

Weiguan Zhang received the Ph.D degree in electronic engineering from the City University of Hong Kong, Hong Kong, in 2014. He is currently an Associate Research Fellow with the School of Mechatronics and Control Engineering, Shenzhen University. His research interests include MEMS sensors, bio-MEMS, flexible tactile sensors, and their applications for human–machine interactions.

Qinhua Guo received the bachelor's degree in optoelectronic information science and engineering from the Guangdong University of Technology, China, in 2019. He is now pursuing the master's degree in optical engineering with Shenzhen University, China. His research interests include flexible electronics, multi-modal sensing systems, micro-nano manufacturing, and advanced functional materials.

Yu Duan received the B.S. degree from the Huazhong University of Science and Technology, China, in 2015, and the master's degree from Shenzhen University, China, in 2019, where he is now pursuing the Ph.D. degree. His research interests are focused on microsensors and flexible electronics.

Chenyang Xing received the Ph.D. degree in inorganic chemistry from the Shanghai Institute of Applied Physics, Chinese Academy of Sciences, China, in 2016. From 2016 to 2018, he worked as a Postdoctoral Researcher with Shenzhen University, where he is currently an Assistant Professor with the School of Physics and Optoelectronic Engineering. His research interests include design, manufacturing, integration of 2D nanomaterials for applications in biomedical application, energy, optoelectronics, and wearable devices.

Zhengchun Peng received the Ph.D. degree in MEMS from the Georgia Institute of Technology, Atlanta, GA, USA. Then, he joined Intel Corporation and worked as a Senior Research and Development Engineer. He is currently a Distinguished Professor with the School of Physics and Optoelectronic Engineering, Shenzhen University. His main research interests are in the fields of micro/nano sensors, flexible and stretchable electronics, their applications in robotics, health monitoring, and human–computer interfaces.